Journal of ELECTRONIC MATERIALS, Vol. 38, No. 1, 2009
DOI: 10.1007/s11664-008-0522-4

Special Issue Paper

Cu-Ni-Sn: A Key System for Lead-Free Soldering

C. SCHMETTERER,[1] H. FLANDORFER,[1,2] CH. LUEF,[1] A. KODENTSOV,[1]
and H. IPSER[1]

1.—Department for Inorganic Chemistry/Materials Chemistry, University of Vienna, Waehringerstr. 42, 1090 Vienna, Austria. 2.—e-mail: hans.flandorfer@univie.ac.at

Being the most complex constituent of the quaternary system Ag-Cu-Ni-Sn, the ternary system Cu-Ni-Sn is the key system for the investigation of the interactions of Ag-Cu-Sn solder alloys with Ni as a contact material. Although this system has been thoroughly studied in the literature, there are still many uncertainties left. In the present work, a study of the phase equilibria in four isothermal sections at 220, 400, 500, and 700°C of the Cu-Ni-Sn system was carried out following a comprehensive literature study. The methods employed were x-ray diffraction (XRD), metallography, and scanning electron microscopy including electron probe microanalysis. The ternary solubilities of the Ni_3Sn_2-Cu_6Sn_5 and Ni_3Sn-Cu_3Sn fields were characterized in detail. So far no continuous solubility between the respective phases has been found. At 25 at.% Sn the existence of two ternary compounds formed from the BiF_3-type $(Cu,Ni)_3Sn$ phase and reported in literature could be confirmed. On the other hand, our results differ significantly from the very recent literature related to lead-free soldering.

Key words: Lead-free solder, phase diagram, Cu-Ni-Sn, phase equilibria, isothermal section

INTRODUCTION

Since lead-free soldering has been implemented in the field of electronics, the quaternary Ag-Cu-Ni-Sn system has become the key system for the understanding of interlayer formation between Ag-Cu-Sn solders (the current industry favorite) and Ni as a substrate material. An accurate description of such a quaternary system, conveniently given by the phase diagram, relies on thorough knowledge of its ternary constituent systems, among them Cu-Ni-Sn. Furthermore, Cu-Ni-Sn alloys themselves are being used as substitutes for conventional Sn-Pb solders in wave soldering, where they are superior to Ag-containing solders in terms of easier handling and cost. Within the discussions about high-temperature (HT) solders for die-attach applications and the development of new solder-related techniques such as transient liquid bonding, Cu-Ni-Sn may once again be one of the key systems. Therefore, this particular ternary system is considered one of the most important systems in the field of soldering, and consequently has been the subject of numerous recent investigations. Previous publications have mainly focused on the (Cu,Ni)-rich part of the system because of the important role of Ni-bronzes with additions of Sn for the electric industry. Recently, focus has shifted to the Sn-rich corner and to lower temperatures within the research field of lead-free solders. Surprisingly, many uncertainties and even misconceptions remain up to this day. As the characteristics of such an alloy system are conveniently summarized by the phase diagram, the aim of the work presented herein was a comprehensive study of this system, represented here by four isothermal sections at 220, 400, 500, and 700°C.

Considering soldering, or even HT soldering purposes, the primary interest may be at temperatures below 400°C. Nevertheless, due to the difficulties in achieving thermodynamic equilibrium at

---

(Received May 7, 2008; accepted July 3, 2008;

such low temperatures it is still worthwhile and useful to determine phase equilibria at higher temperatures. This provides information which can serve as an input into a calculation of phase diagrams (CALPHAD)-type assessment of the alloy system, which again permits a reliable extrapolation to lower temperatures.

LITERATURE REVIEW

The Binary Constituents

In this work, the Cu-Ni binary system was accepted as established by Chakrabarti et al.,[1,2] while the phase equilibria in the Cu-Sn system were taken from the assessment of Saunders and Miodownik.[2,3]

The most recent experimental investigation of the Ni-Sn system was done by Schmetterer et al.[4] Their version of the system differs considerably from the last assessment by Nash and Nash[5] and from two calculated versions of the phase diagram by Ghosh[6] and Liu et al.[7] As a detailed account of all changes in this system can be found in Ref. 4, only the points relevant to the present work will be mentioned.

The Ni_3Sn HT phase was confirmed to have the cubic BiF_3 structure; it is therefore isotypic to Cu_3Sn HT. An orthorhombic βCu_3Ti-type phase could be confirmed to be metastable, formed by a martensitic reaction at high quenching rates.

The region around Ni_3Sn_2 is far more complicated than previously reported. Besides a NiAs-type Ni_3Sn_2 HT-phase there are three corresponding orthorhombic low-temperature (LT) phases, two of which have incommensurate crystal structures. Detailed crystal structure analyses in this region were performed by Leineweber et al.[8–11] The transition between the Ni_3Sn_2 LT and HT phases is first order, consisting of two eutectoid and two peritectoid reactions in the temperature interval between 295°C and 411°C.

The System Cu-Ni-Sn

The ternary Cu-Ni-Sn system was recently comprehensively reviewed by Ghosh[12] covering practically all available literature. Uncertainties can be found in abundance, especially in the sections from Ni_3Sn to Cu_3Sn (25 at.% Sn) and from Ni_3Sn_2 to Cu_6Sn_5 (40–45 at.% Sn). One of the key investigations of the (Cu,Ni)-rich part was done by Wachtel and Bayer[13] who presented a partial isotherm at 650°C and an isopleth at 25 at.% Sn. These authors noticed a stabilization of the BiF_3-type $(Cu,Ni)_3Sn$ phase (γ-phase) to lower temperature and reported a decomposition of this phase resulting in a change of the phase triangulation at Cu-rich concentrations. Lee Pak et al.[14,15] suggested the presence of ternary compounds at Ni-rich concentrations along the Ni_3Sn-Cu_3Sn section. They reported the decomposition of the BiF_3-type $(Cu,Ni)_3Sn$ phase into a βCu_3Ti-type phase (designated 2H). This phase can be formed by two mechanisms, either by massive transformation yielding a thermodynamically stable phase, or martensitically, as described for the binary Ni_3Sn. They furthermore proposed the existence of a distorted βCu_3Ti-type phase having triclinic symmetry (designated d2H) based on electron diffraction experiments. Although the cell parameters are given, neither space group nor atomic arrangement have been determined. However, the authors proposed a detailed mechanism for the formation of this phase.

More recent work focused on temperatures around 240°C due to the application in lead-free soldering, and many experimental and calculated isothermal sections have been suggested in the literature[16–19]; however, all of these studies suffer from a number of shortcomings: the authors reported a solid solution of Cu and Ni in Sn at 240°C, which cannot exist at this temperature above the melting point of Sn. The liquidus, however, was not mentioned at all. Second, although it was recognized that no continuous solid solution between Ni_3Sn LT and Cu_3Sn LT or even Cu_3Sn HT can be formed, the authors still preferred to include it based on the fact that no two- or three-phase region was observed in the scanning electron microscopy (SEM) studies.

Ghosh[12] also mentions a third ternary phase (a Haeusler phase) based on the report by Schreiner et al.[20] However, Wachtel and Bayer[13] could not confirm the existence of such a phase. Oberndorff[21] established an isothermal section at 235°C and reported the existence of a ternary phase $Cu_{27}Ni_{29}Sn_{44}$. Yu et al.[22] performed first-principle calculations along $Cu_{6-x}Ni_xSn_5$ and found an ordering of Cu and Ni atoms at the composition of $Cu_4Ni_2Sn_5$. They assumed $Cu_4Ni_2Sn_5$ to be a ternary intermetallic compound but did not give any information on corresponding phase equilibria or phase transitions. Furthermore, Larsson et al. reported various phases having superstructures of the $InNi_2$-type structure of Cu_6Sn_5 HT.[23,24]

EXPERIMENTAL SECTION

Cu-Ni-Sn alloys were prepared from Cu wire (99.98+%, Goodfellow, UK), Ni wire (grade 1, Speciality Products, Johnson Matthey, Materials Technology, Royston, UK) or Ni sheet (99.99%, Advent Research Materials Ltd., Eynsham—Oxford, UK) and Sn ingots (99.999% metal basis, Ventron Alfa Products, Beverly, MA, USA). The Cu wire was cleaned by heating in a H_2 atmosphere at 250°C.

Calculated amounts of the pure metals were weighed, usually to a total mass of 1–2 g, and alloyed in an electric arc furnace (Edmund Bühler MAM1, Johanna Otto GesmbH, Germany). After alloying all samples were sealed in evacuated quartz tubes and annealed at various temperatures followed by quenching in cold water. Annealing times were usually 9 weeks at or below 400°C, and 6 weeks for the higher temperatures.

Powder XRD data at room temperature were recorded using an Image Plate Guinier camera (Huber GmbH, Rimsting, Germany) on a Siemens Kristalloflex ERL 1000 generator (Siemens AG, Berlin, Germany) with Cu$K_{\alpha1}$ radiation or on a Bruker D8 powder diffractometer. High-purity Si powder mixed with the samples was used as an internal standard. The patterns were analyzed using Topas 3 software (Bruker AXS, Karlsruhe, Germany). Crystal structure data were taken from Pearson's *Handbook of Intermetallic Phases*[25] or from recent publications.[8–11,23,24]

Samples to be examined by SEM were embedded in a mixture of 1:2 volume parts of Cu powder and Resinar F (Wirtz/Buehler, Düsseldorf, Germany) or in graphite-containing conductive polymer. After embedding, the samples were ground with SiC discs with 600 to 1200 mesh and polished with Al_2O_3 (1 μm) to obtain a smooth surface.

Scanning electron microscopy (SEM) and electron probe microanalysis (EPMA) measurements were performed in Vienna [Cameca SX100, Wavelength Dispersive Spectroscopy (WDS); 15 kV/20 nA beam current; ZAF matrix correction] and Eindhoven [JEOL JSM-840A, Energy Dispersive X-ray Spectroscopy (EDX); 20 kV/1–1.5 nA beam current; ZAF correction]. Some of the measurements were done in cooperation with the Department of Physics of Materials, Academy of Sciences of the Czech Republic, in Brno (JEOL JSM-6460, EDX; 15 kV). The pure metals Cu, Ni, and Sn were used for the calibration of the instruments.

RESULTS AND DISCUSSION

Results of the phase analysis based on EPMA and XRD data of samples annealed at 220, 400, 500, and 700°C are summarized in Table I. The isothermal sections drawn from these data are shown in Figs. 1–4. At 220°C (Fig. 4) only the Sn-rich part is based on experimental data, as in the (Cu,Ni)-rich part below 40 at.% Sn equilibrium samples are likely not to be obtained. Thus, the (Cu,Ni)-rich part has been extrapolated from the higher temperatures. The liquidus lines in the isothermal sections (Figs. 1–4) were estimated from the binary systems and a limited number of differential thermal analysis (DTA) measurements.[26]

As expected from the literature study, rather complex phase relations were encountered in the system Cu-Ni-Sn, even more complicated by the formation of metastable phases during quenching and by the existence of HT–LT phase transitions. For example, in the binary Cu-Sn system the γ-phase is known to quickly transform partly or completely into δ or ε on cooling or quenching.[27] This was observed in the ternary system, too, in a number of samples, e.g., $Cu_{40}Ni_{10}Sn_{50}$ or $Cu_{25}Ni_{53}Sn_{22}$ quenched from 700°C. Although this made the interpretation of experimental results rather difficult, a number of uncertainties could be clarified in the present work.

According to the vertical section at 25 at.% Sn published by Wachtel and Bayer,[13] there is a temperature-dependent continuous solid solution between Ni_3Sn HT and Cu_3Sn HT (γ-phase, in the literature also designated "H"). From the binary systems Ni-Sn and Cu-Sn it is evident that this solid solution cannot show up as such in isothermal sections at any temperature, because the two isotypic binary phases are not stable in a common temperature range. Thus a continuous solid solution in an isothermal section at 240°C as shown by Lin et al.[16] can obviously not exist.

According to our findings and in agreement with Wachtel and Bayer,[13] the γ-phase solid solution is stabilized down to lower temperatures over a wide concentration range. Its stability range narrows significantly with decreasing temperature (compare the isothermal sections in Figs. 1–3). On both the Cu- and the Ni-rich sides, respectively, this γ-phase solid solution was found to decompose into several other phases at lower temperature, as has already been recognized in earlier investigations.[13–15]

From our investigations, the decompositions on the Cu-rich side were found to take place between approximately 400°C and 500°C (compare the relevant isothermal sections in Figs. 2 and 3). This temperature range is slightly smaller than indicated by Wachtel and Bayer.[13] Details concerning the reactions involved are the subject of ongoing investigations, but the change in phase equilibria as a result of these decompositions can be recognized from a comparison of the isothermal sections at 400°C (Fig. 3) and 500°C (Fig. 2). While there still exists an extended homogeneity range of the γ-phase at 500°C, various two- and three-phase fields appear at 400°C. They directly connect the (Cu,Ni) solid solution and the two Cu-Sn compounds ε and ζ with ternary solutions based on Ni_3Sn_2 and Cu_6Sn_5. This is in rather good agreement with the results of Wachtel and Bayer,[13] but is in complete contrast to recent work concerning isothermal sections at 235, 240, and 250°C.[16–19,21]

On the Ni-rich side, a βCu_3Ti-type phase designated as "2H" was first reported and identified as a stable phase by Lee Pak et al.[14,15] In the present work, the designation $\tau1$ will be used. It is interesting that in both binary systems, Cu-Sn[3] and Ni-Sn,[4] an isotypic metastable phase is formed at about 25 at.% Sn by rapid cooling out of the γ-phase.

In the present work, the stable ternary phase $\tau1$ was identified by XRD in several samples annealed at 400, 500, and 700°C. The model for the crystal structure given in Table II was used to index the corresponding peaks in the powder diffractograms. It could be confirmed that it is a truly stable equilibrium phase in the ternary Cu-Ni-Sn system, in good agreement with essential literature cited above. Due to its crystal structure, which is different from any other phase in the neighborhood and due to its clear separation from other phases by two- or three-phase fields, this phase is a true ternary

Table I. Experimental Results of the Phase Analysis in the Cu-Ni-Sn System

Nominal Composition, at.%	Heat Treatment, °C	Phase	Structure Type	Lattice Parameters, pm	WDS^{w}/EDX^{e,e*}			
					Cu, at.%	Ni, at.%	Sn, at.%	Σ wt.%
700°C								
$Cu_{83}Ni_2Sn_{15}$	700, 41d	(Cu,Ni)	Cu	a = 369.970(4)	89.8	1.5	8.7	e^*
		β	W	a = 297.993(3)	82.3	2.0	15.7	
		γ	BiF_3	a = 597.43(1)	78.1	2.9	19.1	
$Cu_{80}Ni_5Sn_{15}$	700, 41d	(Cu,Ni)	Cu	a = 369.724(4)	88.5	2.4	9.1	e^*
		δ^{ne}	$Cu_{41}Sn_{11}$	a = 1798.13(8)			Not found	
		γ	BiF_3	a = 598.654(9)	75.0	6.3	18.7	
$Cu_{75}Ni_{10}Sn_{15}$	700, 41d	(Cu,Ni)	Cu	a = 367.770(4)	88.1	4.3	7.6	e^*
		γ	BiF_3	a = 597.385(8)	57.9	18.7	23.4	
$Cu_{70}Ni_{15}Sn_{15}$	700, 42d	(Cu,Ni)	Cu	a = 366.69(3)	88.9	5.3	5.9	101.8^e
		γ	BiF_3	a = 595.71(7)	49.5	26.0	24.5	102.4
$Cu_{50}Ni_{35}Sn_{15}$	700, 42d	(Cu,Ni)	Cu	a = 361.55(3)	81.4	16.6	2.0	103.1^e
		γ	BiF_3	c = 592.80(9)	24.4	50.4	25.1	104.6
$Cu_{25}Ni_{60}Sn_{15}$	700, 42d	(Cu,Ni)	Cu	a = 360.702(2)	39.8	55.0	5.2	101.3
		$\tau1$	βCu_3Ti	a = 536.749(5) b = 428.775(4) c = 451.365(4)	10.2	65.8	24.0	102.3^e
$Cu_{10}Ni_{75}Sn_{15}$	700, 42d	(Cu,Ni)	Cu	a = 358.83(2)	14.7	79.1	6.2	102.6^e
		Ni_3Sn LT	Mg_3Cd	a = 529.21(5) c = 425.96(8)	4.0	72.0	24.0	103.0
$Cu_{25}Ni_{53}Sn_{22}$	700, 41d	(Cu,Ni)	Cu	a = 360.881(7)	64.4	31.7	3.9	e^*
		γ	BiF_3	a = 592.823(5)	18.7	56.0	25.3	
		ε	Cu_3Sn	Traces only				
		$\tau1'$	βCu_3Ti	a = 554.11(2) b = 429.30(2) c = 437.85(2)				
$Cu_{23}Ni_{55}Sn_{22}$	700, 41d	(Cu,Ni)	Cu	a = 360.65(2)	59.5	36.6	3.9	e^*
		γ	BiF_3	a = 591.9(2)	17.8	56.4	25.8	
		ε	Cu_3Sn	a = 554.7(1) b = 424.73(4) c = 451.2(1)				
		$\tau1'$	βCu_3Ti	a = 552.71(2) b = 429.36(1) c = 438.37(2) + a few unindexed lines				
$Cu_{20}Ni_{58}Sn_{22}$	700, 41d	(Cu,Ni)	Cu	a = 360.597(5)	50.5	44.3	5.2	e^*
		γ	BiF_3	a = 591.75(2)	15.5	59.2	25.3	
		$\tau1$	βCu_3Ti	a = 537.600(5) b = 429.312(4) c = 451.415(4)	12.6	63.1	24.3	
$Cu_{50}Ni_{17}Sn_{33}$	700, 42d	γ	BiF_3	a = 598.85(1)	66.5	7.1	26.4	102.7^e
		ε	Cu_3Sn	a = 550.3(2) b = 432.85(6) c = 477.5(2)				
		Ni_3Sn_2 HT	$InNi_2$	a = 416.608(7) c = 515.65(1)	32.9	26.5	40.5	102.6
$Cu_{37}Ni_{30}Sn_{33}$	700, 42d	γ	BiF_3	a = 598.195(7)	54.8	19.5	25.8	101.7^e
		Ni_3Sn_2 HT	$InNi_2$	a = 415.044(4) c = 519.588(8)	21.2	39.7	39.1	101.5
$Cu_{20}Ni_{47}Sn_{33}$	700, 42d	γ	BiF_3	a = 594.40(1)	32.5	41.3	26.2	103.2^e
		Ni_3Sn_2 HT	$InNi_2$	a = 414.007(9) c = 520.72(1)	9.7	51.6	38.7	103.5
$Cu_{10}Ni_{57}Sn_{33}$	700, 42d	γ	BiF_3	a = 588.50(3)	17.0	56.2	26.8	100.2^e
		Ni_3Sn_2 HT	$InNi_2$	a = 413.64(3) c = 520.44(4)	2.9	57.9	39.2	101.1
		$\tau1$	βCu_3Ti	a = 539.0(1) b = 430.4(9) c = 448.8(1)	13.8	59.8	26.4	100.5

Table I. Continued

Nominal Composition, at.%	Heat Treatment, °C	Phase	Structure Type	Lattice Parameters, pm	WDS^w/EDX^{e,e*} Cu, at.%	Ni, at.%	Sn, at.%	Σ wt.%
$Cu_{40}Ni_{10}Sn_{50}$	700, 42d	ε	Cu_3Sn	a = 551.6(1) b = 432.73(4) c = 477.7(1)	73.5	0.0	26.5	98.6^e
		Ni_3Sn_2 HT	$InNi_2$	a = 416.73(1) c = 513.02(2)	34.3	22.3	43.4	100.7
		Cu_6Sn_5 (l)	$InNi_2$	a = 420.34(1) c = 511.15(3)				
		(Sn) (l)	βSn	a = 583.01(1) c = 318.07(1)	1.4	0.0	98.6	101.1
$Cu_{30}Ni_{20}Sn_{50}$	700, 42d	Ni_3Sn_2 HT	$InNi_2$	a = 414.601(7) c = 513.80(1)	30.2	25.4	44.4	100.4^e
		Cu_6Sn_5 (l)	$InNi_2$	a = 420.2(1) c = 510.59(2)				
		(Sn) (l)	βSn	a = 582.91(4) c = 317.79(3)	1.5	0.1	98.4	100.5
$Cu_{20}Ni_{30}Sn_{50}$	700, 42d	Ni_3Sn_2 HT	$InNi_2$	a = 411.850(4) c = 514.371(7)	23.3	31.4	45.3	104.5^e
		(Sn) (l)	βSn	a = 583.03(8) c = 317.99(5)	0.5	0.0	99.5	104.8
$Cu_{10}Ni_{40}Sn_{50}$	700, 42d	Ni_3Sn_2 HT	$InNi_2$	a = 407.774(4) c = 514.132(7)	11.0	43.4	45.6	105.0^e
		Ni_3Sn_4	Ni_3Sn_4	Traces only	3.6	38.4	58.0	104.6
		(Sn) (l)	βSn	a = 583.04(6) c = 317.95(4)	0.0	0.0	100.0	105.3
$Cu_{30}Ni_{10}Sn_{60}$	700, 42d	Ni_3Sn_2 HT	$InNi_2$	a = 414.544(5) c = 513.711(9)	30.6	25.6	43.8	100.4
		Cu_6Sn_5 (l)	$InNi_2$	a = 417.00(6) c = 512.3(1)				
		(Sn) (l)	βSn	a = 582.93(4) c = 317.39(3)	0.6	0.1	99.4	100.2^e
$Cu_{20}Ni_{20}Sn_{60}$	700, 42d	Ni_3Sn_2 HT	$InNi_2$	a = 411.772(5) c = 514.547(8)	23.7	32.5	43.8	101.5^e
		Ni_3Sn_4	Ni_3Sn_4	Not found in XRD	25.9	15.9	58.2	98.1
		Cu_6Sn_5 HT (l)	$InNi_2$	Traces only	43.1	8.2	48.7	100.8
		(Sn) (l)	βSn	a = 582.9(1) c = 317.85(7)	0.2	0.2	99.6	101.2
$Cu_{10}Ni_{30}Sn_{60}$	700, 42d	Ni_3Sn_2 HT	$InNi_2$	a = 408.327(4) c = 514.455(7)	13.0	42.2	44.8	100.7^e
		Ni_3Sn_4	Ni_3Sn_4	Traces only	3.6	38.5	57.9	101.7
		(Sn) (l)	βSn	a = 583.07(7) c = 318.10(5)	1.1	0.7	98.2	100.2
$Cu_{20}Ni_{10}Sn_{70}$	700, 42d	Ni_3Sn_2 HT	$InNi_2$	a = 416.69(1) c = 509.24(3)	25.8	30.1	55.1	100.6^e
		(Sn) (l)	βSn	a = 583.246(4) c = 318.270(3) + weak unindexed lines	1.3	0.1	98.6	98.8
$Cu_{10}Ni_{20}Sn_{70}$	700, 42d	Ni_3Sn_2 HT	$InNi_2$	a = 409.35(2) c = 513.99(3)	16.4	39.2	44.4	100.5^e
		Ni_3Sn_4	Ni_3Sn_4	a = 1223.9(1) b = 408.03(3) c = 525.68(4) β = 105.327(6) deg				
		(Sn) (l)	βSn	a = 583.188(7) c = 318.181(5)	1.3	0.0	98.7	99.2
$Cu_{10}Ni_{10}Sn_{80}$	700, 42d	Ni_3Sn_2 HT	$InNi_2$	a = 411.68(1) c = 511.99(3)	18.7	37.3	44.0	100.5^e
		(Sn) (l)	βSn	a = 583.181(3) c = 318.226(3) + weak Unindexed lines	0.5	0.5	99.0	100.3
500°C								
$Cu_{83}Ni_2Sn_{15}$	500, 55d	(Cu,Ni)	Cu	a = 369.804(1)	90.7	0.5	8.8	98.3^w
		ζ	$Cu_{10}Sn_3$	a = 729.844(3) c = 786.292(5)	73.9	3.6	22.5	100.5
$Cu_{80}Ni_5Sn_{15}$	500, 55d	(Cu,Ni)	Cu	a = 368.352(2)	91.7	1.1	7.2	100.1^w
		ζ	$Cu_{10}Sn_3$	a = 731.674(3) c = 786.730(5)	68.5	8.3	23.3	102.0
$Cu_{75}Ni_{10}Sn_{15}$	500, 55d	(Cu,Ni)	Cu	a = 366.636(3)	92.7	1.6	5.7	100.7^w
		γ	BiF_3	a = 597.810(5)	56.5	18.2	25.3	102.2
$Cu_{70}Ni_{15}Sn_{15}$	500, 42d	(Cu,Ni)	Cu	a = 364.98(3)	93.4	2.6	4.0	99.5^e
		γ	BiF_3	a = 594.96(5)	48.1	25.5	26.3	100.8
$Cu_{50}Ni_{35}Sn_{15}$	500, 42d	(Cu,Ni)	Cu	a = 365.27(3)	87.2	11.7	1.1	98.4^e
		γ	BiF_3	a = 595.77(6)	22.2	51.2	26.6	102.0

Table I. Continued

					WDS^{w}/EDX^{e,e*}			
Nominal Composition, at.%	**Heat Treatment, °C**	**Phase**	**Structure Type**	**Lattice Parameters, pm**	**Cu, at.%**	**Ni, at.%**	**Sn, at.%**	**Σ wt.%**
$Cu_{25}Ni_{60}Sn_{15}$	500, 42d	(Cu,Ni)	Cu	a = 358.06(1)	50.1	47.4	2.6	99.7^{e}
		Ni_3Sn LT	Mg_3Cd	a = 529.72(3) c = 426.15(4)	6.2	68.6	25.2	103
$Cu_{10}Ni_{75}Sn_{15}$	500, 42d	(Cu,Ni)	Cu	a = 356.20(4)	18.1	78.1	3.8	100.7^{e}
		Ni_3Sn LT	Mg_3Cd	a = 529.38(7) c = 425.86(8)	4.3	70.6	25.2	102.6
$Cu_{25}Ni_{53}Sn_{22}$	500, 55d	(Cu,Ni)	Cu	a = 361.50(3)	82.2	13.8	4.0	101.3^{w}
		γ	BiF_3	a = 592.73(1)	19.5	55.8	24.8	101.3
		$\tau1$	βCu_3Ti	a = 539.024(6) b = 430.033(4) c = 451.576(5)				
$Cu_{23}Ni_{55}Sn_{22}$	500, 55d	(Cu,Ni)	Cu	a = 361.12(3)	85.1	13.3	1.6	97.9^{w}
		$\tau1$	βCu_3Ti	a = 540.25(4) b = 430.67(4) c = 450.88(4)	17.8	57.5	24.7	101.0
$Cu_{20}Ni_{58}Sn_{22}$	500, 55d	(Cu,Ni)	Cu	a = 360.11(2)	81.7	16.8	1.5	98.8^{w}
		$\tau1$	βCu_3Ti	a = 537.430(4) b = 429.133(3) c = 451.487(4)	13.8	61.0	25.2	101.0
$Cu_{50}Ni_{17}Sn_{33}$	500, 42d	ε	Cu_3Sn	a = 550.85(6) b = 433.10(2) c = 476.96(6)	70.9	2.4	26.8	100.9^{e}
		Ni_3Sn_2 HT	$InNi_2$	a = 415.84(1) c = 515.53(3) + unindexed lines	28.4	28.6	43.0	102.2
$Cu_{37}Ni_{30}Sn_{33}$	500, 42d	γ	BiF_3	a = 598.543(7)	55.5	17.7	26.9	101.2^{e}
		Ni_3Sn_2 HT	$InNi_2$	a = 414.151(5) c = 519.57(1)	18.8	39.6	41.6	103.0
$Cu_{20}Ni_{47}Sn_{33}$	500, 46d	γ	BiF_3	a = 594.489(7)	32.6	40.2	27.2	101.3^{w}
		Ni_3Sn_2 HT	$InNi_2$	a = 413.203(4) c = 520.295(7)	8.8	51.2	40.1	101.0
$Cu_{10}Ni_{57}Sn_{33}$	500, 46d	γ	BiF_3	a = 592.26(1)	20.3	52.8	26.9	100.8^{w}
		Ni_3Sn_2 HT	$InNi_2$	a = 413.028(5) c = 520.348(8)	4.3	56.3	39.4	100.9
		$\tau1$	βCu_3Ti	a = 539.57(6) b = 430.09(5) c = 451.50(6)	14.8	59.1	26.1	100.8
$Cu_{40}Ni_{10}Sn_{50}$	500, 46d	Ni_3Sn_2 HT	$InNi_2$	a = 418.167(7) c = 511.37(1)	43.4	11.7	44.9	101.9^{w}
		Cu_6Sn_5 HT (l)	$InNi_2$	a = 417.97(4) c = 510.60(9)	53.2	1.5	45.3	101.1
		(Sn) (l)	βSn	a = 582.82(5) c = 317.94(4)	0.2	0.0	99.8	99.9
$Cu_{30}Ni_{20}Sn_{50}$	500, 42d	Ni_3Sn_2 HT	$InNi_2$	Only qualitative phase identification from film XRD patterns	33.4	20.9	45.7	104.1^{e}
		Cu_6Sn_5 HT (l)	$InNi_2$		52.2	0.3	47.5	102.6
		(Sn) (l)	βSn		0.5	0.0	99.5	105.1
$Cu_{20}Ni_{30}Sn_{50}$	500, 42d	Ni_3Sn_2 HT	$InNi_2$	Only qualitative phase identification from film XRD patterns	24.5	29.8	45.7	103.4^{e}
		(Sn) (l)	βSn		0.5	0.0	99.6	104.9
$Cu_{10}Ni_{40}Sn_{50}$	500, 42d	Ni_3Sn_2 HT	$InNi_2$	Only qualitative phase identification from film XRD patterns	15.4	38.9	45.7	103.5^{e}
		Ni_3Sn_4	βSn		2.5	40.8	56.7	104.1
$Cu_{30}Ni_{10}Sn_{60}$	500, 42d	Ni_3Sn_2 HT	$InNi_2$	Only qualitative phase identification from film XRD patterns	36.1	17.8	46.1	103.3^{e}
		Cu_6Sn_5 HT (l)	$InNi_2$		51.2	1.3	47.5	102.7
		(Sn) (l)	βSn		3.0	0.0	97.0	104.5
$Cu_{20}Ni_{20}Sn_{60}$	500, 42d	Ni_3Sn_2 HT	$InNi_2$	Only qualitative phase identification from film XRD patterns	25.9	28.4	45.7	102.8^{e}
		(Sn) (l)	βSn		0.5	0.1	99.4	104.6

Table I. Continued

Nominal Composition, at.%	Heat Treatment, °C	Phase	Structure Type	Lattice Parameters, pm	$\text{WDS}^{w}/\text{EDX}^{e,e*}$			
					Cu, at.%	Ni, at.%	Sn, at.%	Σ wt.%
$Cu_{10}Ni_{30}Sn_{60}$	500, 46d	Ni_3Sn_2 HT	$InNi_2$	a = 409.81(1) c = 513.44(2)	21.6	32.7	45.6	100.9^{w}
		Ni_3Sn_4	Ni_3Sn_4	a = 1225.36(6) b = 407.14(2) c = 523.66(3) β = 105.081(4) deg	3.7	38.2	58.1	100.7
		(Sn) (l)	βSn	a = 583.18(2) c = 317.99(2) from liquid	0.2	0.1	99.7	99.0
$Cu_{20}Ni_{10}Sn_{70}$	500, 42d	Ni_3Sn_2 HT	$InNi_2$	a = 414.31(1) c = 511.20(2)	30.9	23.5	45.6	103.4^{e}
		Cu_6Sn_5 HT (l)	$InNi_2$	Not found in XRD	39.1	13.8	47.1	102.1
		(Sn) (l)	βSn	a = 583.155(7) c = 318.216(5)	0.2	0.1	99.7	103.5
$Cu_{10}Ni_{20}Sn_{70}$	500, 42d	Ni_3Sn_2 HT	$InNi_2$	a = 409.51(3) c = 513.59(7)	18.1	35.7	46.1	103.0^{e}
		Ni_3Sn_4	Ni_3Sn_4	a = 1217.8(2) b = 409.02(8) c = 521.2(1) β = 104.59(2) deg	3.3	39.3	57.4	104.1
		Cu_6Sn_5 HT (l)	$InNi_2$	a = 422.4(2) c = 512.2(4)	25.3	27.6	47.1	103.1
		(Sn) (l)	βSn	a = 583.18(1) c = 318.217(7)	0.4	0.2	99.4	104.5
$Cu_{10}Ni_{10}Sn_{80}$	500, 42d	Ni_3Sn_2 HT	$InNi_2$	a = 411.43(2) c = 512.25(4)	22.9	31.5	45.7	103.6^{e}
		Cu_6Sn_5 HT (l)	$InNi_2$	Not found in XRD	29.4	23.6	47.0	102.6
		(Sn) (l)	βSn	a = 583.168(5) c = 318.212(4)	0.0	0.2	99.8	104.7
$Cu_5Ni_5Sn_{90}$	500, 42d	Ni_3Sn_2 HT	$InNi_2$	a = 411.76(2) c = 511.19(3)	24.4	29.9	45.7	103.2^{e}
		Cu_6Sn_5 HT (l)	$InNi_2$	Not found in XRD	19.8	34.1	46.1	103.5
		(Sn) (l)	βSn	a = 583.150(3) c = 318.243(2)	0.6	0.1	99.3	104.9
400°C								
$Cu_{83}Ni_2Sn_{15}$	400, 63d	(Cu,Ni)	Cu	a = 367.811(2)	92.7	0.2	7.1	100.3^{w}
		ζ	$Cu_{10}Sn_3$	a = 731.930(3) c = 786.633(4)	73.4	3.7	22.8	102.6
$Cu_{80}Ni_5Sn_{15}$	400, 63d	(Cu,Ni)	Cu	a = 365.544(2)	93.4	1.2	5.4	100.1^{w}
		ζ	$Cu_{10}Sn_3$	a = 729.994(3) c = 786.320(4)	68.5	8.0	23.5	102.2
$Cu_{75}Ni_{10}Sn_{15}$	400, 63d	(Cu,Ni)	Cu	a = 365.159(2)	84.9	6.0	9.1	101.2^{w}
		ζ	$Cu_{10}Sn_3$	a = 729.716(7) c = 786.267(9)	67.3	9.3	23.4	102.5
		Ni_3Sn_2 LT	Ni_3Sn_2	a = 711.07(3) b = 519.55(2) c = 829.12(4)	20	40.5	39.5	102.4
$Cu_{25}Ni_{53}Sn_{22}$	400, 63d	(Cu,Ni)	Cu	a = 360.47(5)	46.2	45.5	8.3	100.4^{w}
		γ	BiF_3	a = 593.14(2)	23.2	50.1	26.7	101.0
		$\tau1$	βCu_3Ti	a = 539.951(8) b = 430.503(6) c = 451.457(7)	17.2	56.9	25.9	101.1
$Cu_{23}Ni_{55}Sn_{22}$	400, 63d	(Cu,Ni)	Cu	a = 360.19(5)	42.8	48.8	8.3	99.9^{w}
		γ	BiF_3	a = 593.20(5)	23.1	50.0	26.8	101.1
		$\tau1$	βCu_3Ti	a = 539.584(9) b = 430.305(7) c = 451.488(7)	15.7	58.7	25.6	101.5
$Cu_{20}Ni_{58}Sn_{22}$	400, 63d	(Cu,Ni)	Cu	a = 359.91(6)	35.1	56.0	8.9	100.5^{w}
		$\tau1$	βCu_3Ti	a = 538.77(1) b = 429.868(7) c = 451.543(8)	15.3	59.1	25.6	101.1
$Cu_{15.5}Ni_{62}Sn_{22.5}$	400, 63d	(Cu,Ni)	Cu	a = 360.6(1)	25.1	65.3	9.6	100.6^{w}
		$\tau1$	βCu_3Ti	a = 537.75(1) b = 429.35(1) c = 451.59(9)	12.1	62.6	25.3	101.4
$Cu_{8.1}Ni_{69.4}Sn_{22.5}$	400, 42d	(Cu,Ni)	Cu	a = 361.64(5)				
		Ni_3Sn LT	Mg_3Cd	a = 529.99(2) c = 426.90(3)				
		$\tau1$	βCu_3Ti	a = 534.64(9) b = 428.47(7) c = 451.20(8)				
$Cu_{1.8}Ni_{76}Sn_{22.2}$	400, 42d	(Cu,Ni)	Cu	a = 353.31(6)				
		Ni_3Sn LT	Mg_3Cd	a = 529.21(1) c = 425.06(2)				

Table I. Continued

Nominal Composition, at.%	Heat Treatment, °C	Phase	Structure Type	Lattice Parameters, pm	WDS[w]/EDX[e,e*]			
					Cu, at.%	Ni, at.%	Sn, at.%	Σ wt.%
$Cu_{42.4}Ni_{33.2}Sn_{24.5}$	400, 42d	(Cu,Ni)	Cu	a = 361.600(8)				
		γ	BiF_3	a = 590.26(5)				
		ε	Cu_3Sn	Traces only				
		Ni_3Sn_2 LT	Ni_3Sn_2	a = 710.93(3) b = 518.91(2) c = 827.22(6)				
$Cu_{31.3}Ni_{44.3}Sn_{24.3}$	400, 42d	(Cu,Ni)	Cu	a = 361.7(1)				
		γ	BiF_3	a = 593.047(9)				
$Cu_{20}Ni_{47}Sn_{33}$	400, 63d	γ	BiF_3	a = 592.88(1)				
		Ni_3Sn_2 HT	$InNi_2$	a = 413.029(7) c = 517.75(2)	11.4	49.6	39.0	101.7[w]
		$\tau 2$		a = 542.36(2) b = 451.07(1) c = 427.92(2) α = 84.373(3) deg β = 85.560(3) deg γ = 84.007(3) deg	27.0	46.0	27.0	101.1
		$\tau 1'$	βCu_3Ti	a = 543.2(1) b = 421.0(1) c = 440.2(1)				
$Cu_{10}Ni_{57}Sn_{33}$	400, 63d	γ	BiF_3	a = 592.87(4)	21.5	51.8	26.8	101.3[w]
		Ni_3Sn_2 HT	$InNi_2$	a = 412.972(5) c = 520.199(8)	4.6	55.9	39.5	101.3
		$\tau 1$	βCu_3Ti	a = 540.14(4) b = 430.77(3) c = 451.26(4)	16.8	57.4	25.9	101.4
$Cu_{4.6}Ni_{58.9}Sn_{36.6}$	400, 42d	Ni_3Sn_2 HT	$InNi_2$	a = 413.065(4) c = 520.110(7)				
		$\tau 1$	βCu_3Ti	a = 539.27(6) b = 430.04(5) c = 452.01(7)				
$Cu_{4.5}Ni_{59}Sn_{36.5}$	400, 63d	Ni_3Sn_2 HT	$InNi_2$	a = 412.751(5) c = 520.081(8)	3.4	57.6	39.0	101.3[w]
		$\tau 1$	βCu_3Ti	a = 538.91(5) b = 429.89(5) c = 451.60(6)	13.1	61.0	25.9	100.6
$Cu_{13.9}Ni_{48.9}Sn_{37.2}$	400, 42d	Ni_3Sn_2 HT	$InNi_2$	a = 413.15(1) c = 518.69(2)				
		$\tau 2$		a = 541.64 b = 450.53 c = 428.24 α = 84.294 deg β = 85.689 deg γ = 83.995 deg				
$Cu_{36.7}Ni_{23.7}Sn_{39.6}$	400, 42d	ε	Cu_3Sn	a = 515.50(8) b = 433.00(4) c = 477.4(1)				
		Cu_6Sn_5 HT	$InNi_2$	a = 414.261(9) c = 513.31(1) or Ni_3Sn_2 HT				
$Cu_{40}Ni_{10}Sn_{50}$	400, 63d	Cu_6Sn_5 HT	$InNi_2$	a = 418.045(9) c = 510.39(2)	44.9	9.4	45.7	101.8[w]
		(Sn) (l)	βSn	a = 583.18(6) c = 318.17(5)	0.9	0.1	99.0	99.2
$Cu_{10}Ni_{30}Sn_{60}$	400, 63d	Cu_6Sn_5 HT	$InNi_2$	a = 410.614(8) c = 512.10(1)	26.0	28.6	45.4	101.5[w]
		Ni_3Sn_4	Ni_3Sn_4	a = 1222.69(3) b = 407.28(1) c = 524.18(1) β = 105.288(2) deg	5.2	36.5	58.3	101.3
		(Sn) (l)	βSn	a = 583.21(1) c = 318.21(1)	0.3	0.5	99.2	99.6
$Cu_{11.5}Ni_{38.2}Sn_{50.3}$	400, 42d	Cu_6Sn_5 HT	$InNi_2$	a = 410.62(2) c = 512.17(3)				
		Ni_3Sn_2 LT′	Incomm.					
		Ni_3Sn_4	Ni_3Sn_4	a = 1223.17(3) b = 407.310(9) c = 524.22(1) β = 105.294(2) deg				
		(Sn) (l)	βSn	a = 583.32(2) c = 318.21(1)				
$Cu_{7.6}Ni_{38.7}Sn_{53.8}$	400, 42d	Ni_3Sn_4	Ni_3Sn_4	a = 1222.88(2) b = 407.327(8) c = 524.21(1) β = 105.300(1) deg				
		Ni_3Sn_2 LT	Ni_3Sn_2	a = 711.90(3) b = 512.02(1) c = 820.67(4)				
		(Sn) (l)	βSn	a = 583.34(2) c = 318.19(1)				
$Cu_{1.9}Ni_{44.9}Sn_{53.3}$	400, 42d	Ni_3Sn_4	Ni_3Sn_4	a = 1221.66(2) b = 406.722(7) c = 523.32(1) β = 105.280(1) deg				
		Ni_3Sn_2 LT or LT′		a = 698.9(6) b = 515.7(2) c = 808.1(7) (for LT)				
		(Sn) (l)	βSn	a = 583.20(1) c = 318.20(1)				

Table I. Continued

Nominal Composition, at.%	Heat Treatment, °C	Phase	Structure Type	Lattice Parameters, pm	WDS^{w}/EDX^{e,e*} Cu, at.%	Ni, at.%	Sn, at.%	Σ wt.%
$Cu_{50}Ni_{5.5}Sn_{44.5}$	400, 63d	Cu_6Sn_5 HT	$InNi_2$	a = 419.99(1) c = 510.84(2)	50.0	4.7	45.3	101.7
$Cu_{49.6}Ni_{5.8}Sn_{44.6}$	400, 42d	Cu_6Sn_5 HT	$InNi_2$	a = 419.788(8) c = 510.72(1)				
$Cu_{40}Ni_{16}Sn_{44}$	400, 63d	ε	Cu_3Sn	Traces only	73.3	0.8	25.9	101.8
		Cu_6Sn_5 HT	$InNi_2$	a = 416.88(1) c = 511.28(2)	40.6	14.4	45.0	101.6
$Cu_{30}Ni_{26.5}Sn_{43.5}$	400, 63d	ε	Cu_3Sn	Traces only	73.5	0.5	26.0	101.4
		Cu_6Sn_5 HT	$InNi_2$	a = 413.441(4) c = 512.471(6)	31.1	24.4	44.5	101.6
$Cu_{28.8}Ni_{28.1}Sn_{43.1}$	400, 42d	ε	Cu_3Sn	Traces only				
		Cu_6Sn_5 HT	$InNi_2$	a = 414.171(9) c = 512.78(1)				
$Cu_{20}Ni_{37.5}Sn_{42.5}$	400, 63d	ζ	$Cu_{10}Sn_3I$	a = 733.3(2) c = 781.7(5)	Not found in EPMA			
		Cu_6Sn_5 HT	$InNi_2$	a = 412.04(1) c = 514.84(2)	23.1	33.1	43.8	101.4
		Ni_3Sn_2 HT	$InNi_2$	a = 411.19(1) c = 516.29(2)	16.5	40.7	42.8	101.5^{w}
$Cu_{18.9}Ni_{38.6}Sn_{42.5}$	400, 42d	ζ	$Cu_{10}Sn_3$	a = 732.4(1) c = 766.0(3)				
		Cu_6Sn_5 HT	$InNi_2$	a = 409.73(1) c = 515.65(2)				
		Ni_3Sn_2 HT	$InNi_2$	a = 410.818(7) c = 512.87(1)				
$Cu_{10}Ni_{48}Sn_{42}$	400, 63d	Ni_3Sn_2 HT	$InNi_2$	a = 408.949(9) c = 516.326(1)	Concentration gradient			
		Ni_3Sn_4	Ni_3Sn_4	a = 1250.8(1) b = 423.43(3) c = 497.25(3) β = 105.817(6) deg	1.7	42.1	56.2	101.2
$Cu_5Ni_{53.5}Sn_{41.5}$	400, 63d	Ni_3Sn_2 LT′	Incomm.		4.1	53.3	42.6	101.5^{w}
220°C								
$Cu_{50}Ni_{5.5}Sn_{44.5}$	220, 63d	ε	Cu_3Sn	a = 551.8(8) b = 433.0(2) c = 478.6(8)	73.9	0.0	26.1	101.1^{w}
		Cu_6Sn_5 HT	$InNi_2$	a = 419.55(1) c = 510.37(2)	46.5	7.7	45.8	101.5
$Cu_{40}Ni_{16}Sn_{44}$	220, 63d	Cu_6Sn_5 HT	$InNi_2$	a = 416.88(1) c = 511.28(2)	41.0	13.8	45.2	101.7^{w}
$Cu_{30}Ni_{26.5}Sn_{43.5}$	220, 63d	ε	Cu_3Sn	a = 556.97(5) b = 427.09(2) c = 470.89(5)				
		Cu_6Sn_5 HT	$InNi_2$	a = 414.29(2) c = 511.99(3)	Concentration gradient			
$Cu_{20}Ni_{37.5}Sn_{42.5}$	220, 63d	Cu_6Sn_5 HT	$InNi_2$	a = 412.60(2) c = 512.10(5)	29.6	25.0	45.4	101.2^{w}
		Ni_3Sn_2 (LT or LT′)		a = 711.85(7) b = 517.67(3) c = 820.02(8)	12.4	45.4	42.2	100.9
		Ni_3Sn_4	Ni_3Sn_4	a = 1237.7(5) b = 414.7(1) c = 536.2(2) β = 103.72(2) deg	5.8	36.4	57.8	100.7
$Cu_{10}Ni_{48}Sn_{42}$	220, 63d	Ni_3Sn_2 (LT or LT′)		a = 711.84(3) b = 517.34(2) c = 817.93(5) (for LT)	6.9	51.1	42.0	100.3^{w}
		Ni_3Sn_4	Ni_3Sn_4	a = 1224.4(3) b = 408.24(1) c = 518.33(1) β = 105.06(2) deg				
$Cu_5Ni_{53.5}Sn_{41.5}$	220, 63d	Ni_3Sn_2 (LT or LT′)		a = 710.34(2) b = 518.02(1) c = 815.90(3) (for LT)	4.7	53.0	42.3	100.4^{w}
		Ni_3Sn_4	Ni_3Sn_4	a = 1239.8(6) b = 412.8(2) c = 513.4(2) β = 105.06(4) deg	3.9	38.6	57.5	101.0
$Cu_{40}Ni_{10}Sn_{50}$	220, 63d	Cu_6Sn_5 HT	$InNi_2$	a = 416.611(9) c = 509.12(1)	43.4	10.8	45.8	101.4^{w}
		(Sn)	βSn	a = 583.10(6) c = 318.18(5)	0.7	0.2	99.1	99.8
$Cu_{10}Ni_{40}Sn_{50}$	220, 63d	Ni_3Sn_2 LT′	Incomm.		8.2	47.6	44.2	99.7^{w}
		Ni_3Sn_4	Ni_3Sn_4	a = 1223.64(4) b = 407.15(1) c = 524.02(2) β = 105.228(2) deg	5.2	36.6	58.2	100.8
		Cu_6Sn_5 HT	$InNi_2$	a = 410.04(3) c = 514.39(4)				

Table I. Continued

Nominal Composition, at.%	Heat Treatment, °C	Phase	Structure Type	Lattice Parameters, pm	WDS^{w}/EDX^{e,e*}			
					Cu, at.%	Ni, at.%	Sn, at.%	Σ wt.%
$Cu_{20}Ni_{20}Sn_{60}$	220, 63d	Cu_6Sn_5 HT	$InNi_2$	a = 411.72(1) c = 510.19(2)	30.3	24.1	45.6	100.3^{e}
		Ni_3Sn_4	Ni_3Sn_4	a = 1223.4(1) b = 407.86(4) c = 525.13(5) β = 105.330(8) deg	8.5	34.0	57.6	100.5
		(Sn)	βSn	a = 583.26(1) c = 318.125(9)	1.3	1.0	97.7	101.0
$Cu_{15}Ni_{25}Sn_{60}$	220, 63d	Cu_6Sn_5 HT	$InNi_2$	a = 410.47(1) c = 512.16(2)	26.1	28.3	45.6	100.9^{w}
		Ni_3Sn_4	Ni_3Sn_4	a = 1223.6(1) b = 407.57(4) c = 524.73(5) β = 105.386(8) deg	5.6	36.1	58.3	100.5
		(Sn)	βSn	a = 583.30(2) c = 318.23(1)	0.5	1.0	98.5	100.0^{e}
$Cu_{10}Ni_{30}Sn_{60}$	220, 63d	Cu_6Sn_5 HT	$InNi_2$	a = 411.70(2) c = 510.31(4)	Grains too small for measurement			
		Ni_3Sn_4	Ni_3Sn_4	a = 1223.35(5) b = 407.86(1) c = 525.07(2)	8.5	32.8	58.7	102.9
		(Sn)	βSn	a = 583.16(2) c = 318.20(1)	2.0	2.7	95.3	104.0
$Cu_{20}Ni_{10}Sn_{70}$	220, 63d	Cu_6Sn_5 HT	$InNi_2$	a = 413.933(5) c = 509.37(1)	0.7	0.3	99.0	103.6^{e}
		(Sn)	βSn	a = 583.188(5) c = 318.332(4)	34.5	16.7	48.8	101.3^{e}
$Cu_{10}Ni_{20}Sn_{70}$	220, 63d	Cu_6Sn_5 HT	$InNi_2$	a = 411.81(1) c = 510.45(2)	Grains too small for measurement			
		Ni_3Sn_4	Ni_3Sn_4	a = 1224.24(5) b = 408.00(1) c = 525.44(2) β = 105.302(3) deg	6.7	33.7	59.5	103.6
		(Sn)	βSn	a = 583.206(6) c = 318.300(5)	0.6	0.6	98.8	102.7
$Cu_{10}Ni_{10}Sn_{80}$	220, 63d	Cu_6Sn_5 HT	$InNi_2$	a = 412.16(1) c = 510.35(2)	21.1	33.8	45.2	98.3^{e}
		Ni_3Sn_4	Ni_3Sn_4	a = 1224.9(1) b = 408.17(7) c = 525.37(8) β = 105.29(1) deg	7.8	33.5	58.7	99.1
		(Sn)	βSn	a = 583.171(3) c = 318.287(3)				
$Cu_5Ni_5Sn_{90}$	220, 63d	Cu_6Sn_5 HT	$InNi_2$	a = 412.17(2) c = 510.46(3)	30.1	23.9	46.0	98.3^{e}
		Ni_3Sn_4	Ni_3Sn_4	Traces only	8.5	33.7	57.9	98.6
		(Sn)	βSn	a = 583.207(3) c = 318.272(2)	0.3	0.4	99.3	99.3

Legend: (l) = solidified from liquid during quenching; d = days; ne = nonequilibrium; phase formed during quenching; e* = EDX at ASCR, Brno; e = EDX at TUe, Eindhoven w = WDS at University of Vienna, Vienna.

Phase designations: β = $Cu_{17}Sn_3$; γ = Cu_3Sn HT, also ternary solubility; δ = $Cu_{41}Sn_{11}$; ε = Cu_3Sn LT; ζ = $Cu_{10}Sn_3$; $\tau1$ = ternary βCu_3Ti-type phase; $\tau2$ = ternary triclinic, distorted βCu_3Ti-type phase; $\tau1'$ = ternary martensitic βCu_3Ti-type phase.

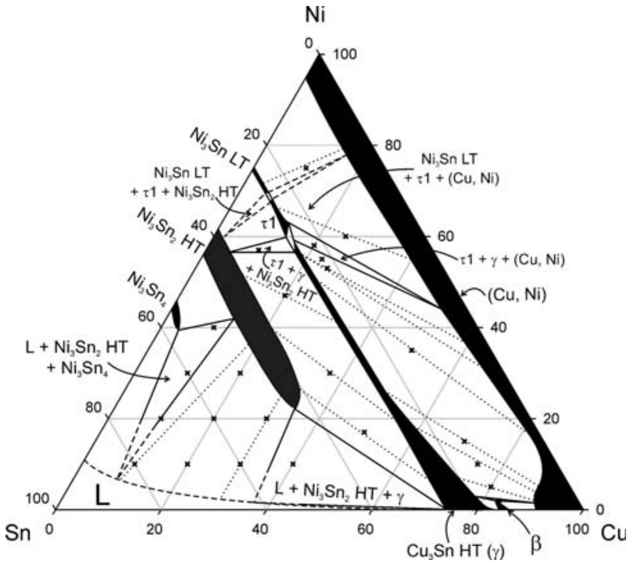

Fig. 1. Cu-Ni-Sn isothermal section at 700°C; axes in at.%. Sample positions are indicated by small crosses; experimentally determined tie lines are shown using *dotted lines* and estimated phase field boundaries are given by *dashed lines*.

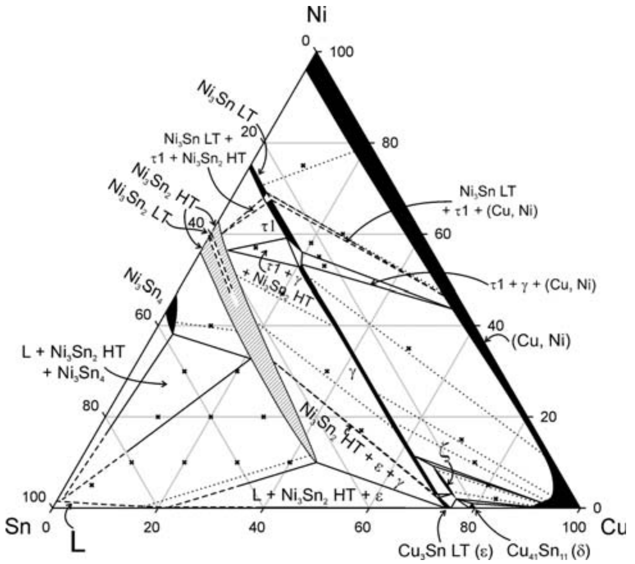

Fig. 2. Cu-Ni-Sn isothermal section at 500°C; axes in at.%. Sample positions are indicated by *small crosses*; experimentally determined tie lines are shown using *dotted lines* and estimated phase field boundaries are given by *dashed lines*.

compound and not a ternary solution of a binary phase (as is the case, e.g., with the γ-phase).

A metastable martensitic transformation yielding a βCu_3Ti-type phase occurs as well in the ternary solution of the γ-phase. In samples placed at $Cu_{25}Ni_{53}Sn_{22}$ and $Cu_{23}Ni_{55}Sn_{22}$ that were quenched from 700°C a phase with a βCu_3Ti-type crystal structure was found in addition to the equilibrium phases. However, its cell dimensions and free parameters of the atom positions (also given in Table II) differ significantly from those of the $\tau 1$

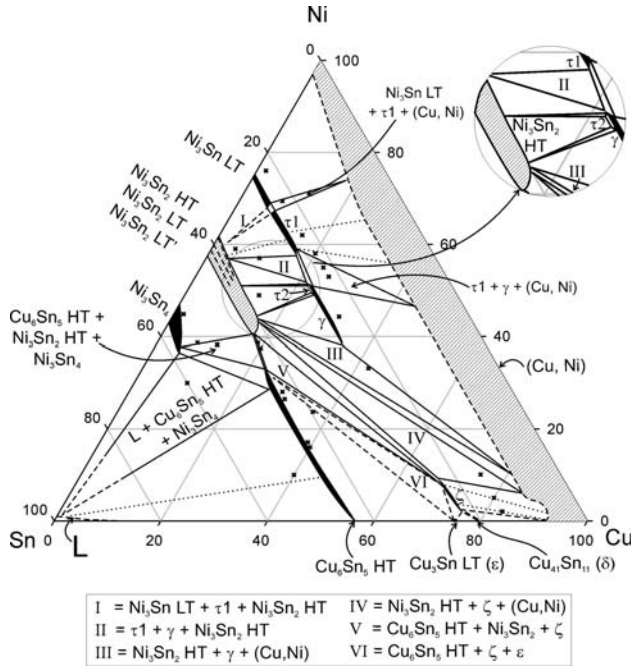

Fig. 3. Cu-Ni-Sn isothermal section at 400°C; axes in at.%. Sample positions are indicated by *small crosses*; experimentally determined tie lines are shown using *dotted lines* and estimated phase field boundaries are given by *dashed lines*. The Ni_3Sn_2 area is shown *shaded*, while the unusually large (Cu,Ni) ternary solubility is shown *shaded and surrounded by a dashed phase boundary*.

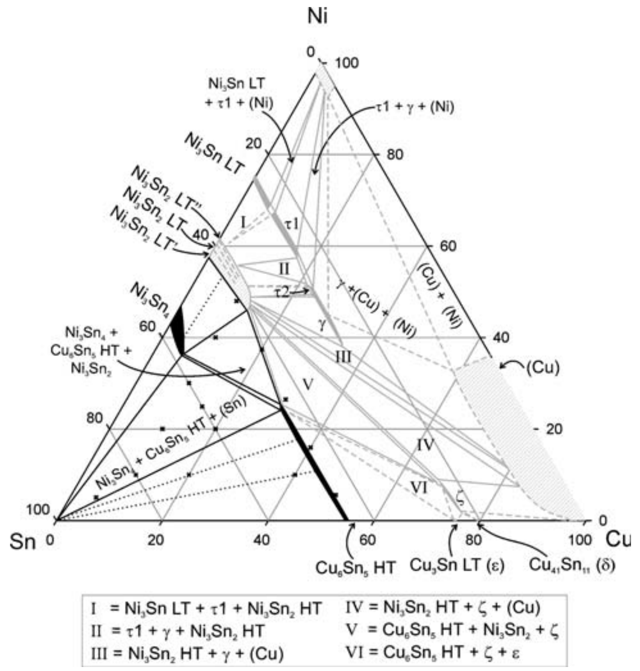

Fig. 4. Cu-Ni-Sn isothermal section at 220°C; axes in at.%. Sample positions are indicated by *small crosses*; experimentally determined tie lines are shown using *dotted lines* and estimated phase field boundaries are given by *dashed lines*. Only the Sn-rich part of this isotherm is based on experiments. The (Cu,Ni)-rich area estimated from the higher temperatures and from the binary systems is shown in *light grey*.

Table II. Comparison of Some Crystallographic Data of the Stable and Metastable βCu$_3$Ti-Type Phases in Cu-Ni-Sn; Space Group for Both Structures: *Pmmn*

τ1 (Stable)		$\tau 1'$ (Metastable)	
Lattice Parameters, pm	**Atomic Positions**	**Lattice Parameters, pm**	**Atomic Positions**
a = 537.60	Sn: 0, 0, 0.82499	a = 554.11	Sn: 0, 0, 0.74895
b = 429.31	Cu/Ni 1: 0, 0.5, 0.19308	b = 429.30	Cu/Ni 1: 0, 0.5, 0.29443
c = 451.42	Cu/Ni 2: 0.25, 0, 0.31865	c = 437.85	Cu/Ni 2: 0.25, 0, 0.18735

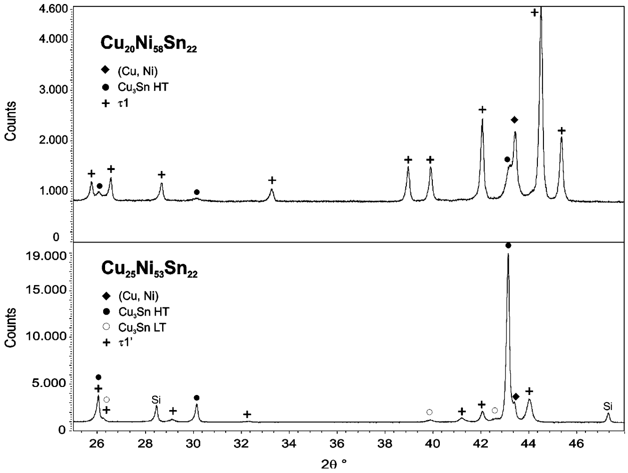

Fig. 5. Diffractograms from Guinier-XRD of samples $Cu_{20}Ni_{58}Sn_{22}$ and $Cu_{25}Ni_{53}Sn_{22}$ including the τ1 and $\tau 1'$ phases, respectively. The powder of the hard samples had to be produced by filing followed by stress annealing.

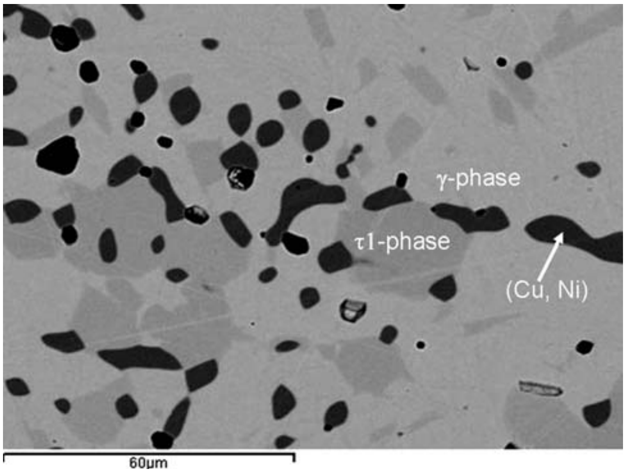

Fig. 6. SEM image of the microstructure of sample $Cu_{20}Ni_{58}Sn_{22}$ quenched from 700°C clearly showing three phases: γ (*light grey*), τ1 (*medium grey*), and (Cu,Ni) solid solution (*dark grey*); the *black spots* are holes.

equilibrium phase. The diffractograms of samples $Cu_{20}Ni_{58}Sn_{22}$ and $Cu_{25}Ni_{53}Sn_{22}$ containing the stable τ1 and $\tau 1'$ phases, respectively, are shown in Fig. 5. It can be seen that peak positions and relative intensities of τ1 and $\tau 1'$ differ significantly. This observation is quite remarkable, as the differences between the lattice parameters and atom positions (cf. Table II) allow a clear distinction between the stable τ1 and the metastable phase designated $\tau 1'$ in this work. These structural changes cannot be explained only by differences in the Cu/Ni ratio, and therefore this phase is considered to be metastable. Its appearance was explained by Lee Pak et al.[14,15]: according to them an alternative, stress-induced martensitic way of formation of the $\tau 1'$ phase out of the γ-phase is possible.

Lee Pak et al.[14,15] described an additional stable phase next to the 25 at.% Sn section. This phase was reported to be a triclinic distortion of the τ1 phase (designated d2H by the authors). In two samples at $Cu_{13.9}Ni_{48.9}Sn_{37.2}$ and $Cu_{20}Ni_{47}Sn_{33}$, quenched from 400°C, a diffraction pattern was observed which could be indexed using either *P1* or *P-1* symmetry and the lattice parameters a = 542.36(2) pm, b = 451.07(1) pm, c = 427.92(2) pm, α = 84.373(3) deg, β = 85.560(3) deg, γ = 84.007(3) deg, starting from the values given by Lee Pak et al.[14,15] However, the available crystallographic data had originally been derived from electron diffraction without any information concerning the atomic positions. Thus we do not consider our powder pattern refinement based on the cell dimensions only and without any atomic positions as a valid proof for the existence of this phase. However, in the sample at $Cu_{10}Ni_{57}Sn_{33}$ the Sn content of 27 at.% obtained by EPMA deviates slightly from the values which were found for the γ-phase in other samples. Therefore, this phase was included as a stable ternary compound in our phase diagram description (designated τ2).

Thus, there are two ternary compounds in the system Cu-Ni-Sn, τ1 and τ2, situated around 25 at.% Sn in addition to the γ-, Ni_3Sn LT, and Cu_3Sn LT phases (Fig. 3). Furthermore, there is the metastable $\tau 1'$ variant of the τ1 phase, fully in agreement with the results of Lee Pak et al.[14,15]

The phase triangulation in the (Cu,Ni)-rich part up to 40 at.% Sn at 700, 500, and 400°C was derived from XRD and EPMA measurements. As an example the micrograph of a sample $Cu_{20}Ni_{58}Sn_{22}$ annealed at 700°C is shown in Fig. 6. Three phases can be distinguished, i.e., the (Cu,Ni) solid solution, τ1 and γ. On the other hand a complementary three-phase field [Ni_3Sn_2 HT + γ + τ1] was found in a sample $Cu_{10}Ni_{57}Sn_{33}$, a composition situated on the Sn-rich side of the [γ + τ1] two-phase field. These results clearly indicate that τ1 is a stable equilibrium phase. In principle, the same phase triangulation concerning γ and τ1 was found at 500°C and 400°C and was accordingly included in Figs. 1–3. At 700°C and 400°C, the orientation of the three-phase fields nicely agrees with the surrounding tie lines also determined by EPMA, whereas at 500°C the concentrations for the (Cu,Ni) phase obtained from the EPMA measurements of samples $Cu_{25}Ni_{53}Sn_{22}$, $Cu_{23}Ni_{55}Sn_{22}$, and $Cu_{20}Ni_{58}Sn_{22}$ turned out to be inconsistent with the lattice parameter variation and with data from other temperatures. Therefore, the (Cu,Ni) apex of the three-phase field [(Cu,Ni) + γ + τ1] at 500°C was placed in consistency with other data and does not reflect the EPMA results.

The phase equilibria around τ1 and γ in principle agree with the thermodynamic modeling by Miettinen[29] who included the ternary phase $Cu_3Ni_{27}Sn_{10}$ (called Γ1; it is identical to τ1 from the present work) in his dataset. The phase triangulation is quite similar except for the placement of the (Cu,Ni)-apex of the three-phase field [(Cu,Ni) + τ1 + γ]: at 700°C there is a small deviation from the present results, while at 550°C this point is placed at a high Cu content in disagreement with the present evaluation (see above). Further work will obviously be needed to clarify this point.

The phase equilibria between Ni_3Sn LT and τ1 are based on the literature information and a limited number of data from the present work (Table I). At 700°C the three-phase field [Ni_3Sn LT + τ1 + (Cu,Ni)] was placed according to the evaluation of the phase equilibria at 800°C from Wang and Chen,[30] whereas at 500°C (Fig. 2) the (Cu,Ni)-apex of this three-phase field was placed in consistency with the experimentally determined tie line Ni_3Sn LT + (Cu,Ni) from EPMA measurements of a sample placed at $Cu_{25}Ni_{60}Sn_{15}$. This, however, was again found to be inconsistent with the data from higher and lower temperatures (Figs. 1 and 3).

The phase triangulation at 400°C (Fig. 3) associated with the τ2 phase is based on the present results (compare results for samples $Cu_{10}Ni_{57}Sn_{33}$ and $Cu_{20}Ni_{47}Sn_{33}$ in Table I), however, it is slightly different from the version given by Lee Pak et al.[15] In the present work, no three-phase field [τ1 + τ2 + γ] could be observed, but rather the three-phase fields [Ni_3Sn_2 HT + γ + τ1] and [Ni_3Sn_2 HT + γ + τ2]. Therefore, we prefer to (tentatively) show two three-phase fields [Ni_3Sn_2 HT + γ + τ2], one on either side of the τ2 phase (Fig. 3).

In the binary Cu-Sn system, there exist a number of phases with a higher Cu content than that of Cu_3Sn HT (γ-phase). At 700°C results obtained from the phase analysis allowed the evaluation of the narrow three-phase field [(Cu,Ni) + β + γ]. Its placement nicely agrees with the thermodynamic modeling of this area from Miettinen.[29] The appearance of $Cu_{41}Sn_{11}$ (δ-phase) in the $Cu_{80}Ni_5Sn_{15}$ sample is considered to be a nonequilibrium effect based on the fact that in the binary Cu-Sn system $Cu_{41}Sn_{11}$ is formed out of Cu_3Sn HT during quenching.[27]

In Cu-rich samples quenched from 400°C to 500°C the phase $Cu_{10}Sn_3$ (ζ-phase) was found by XRD and EDX/EPMA well below its binary thermal stability range (Figs. 2 and 3). This observation suggests a stabilization of this phase to lower temperature, similar to the γ-phase, and is consistent with the report of Wachtel and Bayer.[13] The corresponding three-phase fields on the Cu-rich side have to be very narrow and therefore could not be observed experimentally. There is a remarkable ternary solubility of approximately 9 at.% Ni in the ζ-phase, whereas the Cu_3Sn LT phase (ε-phase) shows only minor solubility of Ni (2 at.% maximum).

The solubility of Sn in (Cu,Ni) was found to decrease slightly from 700°C to 500°C (compare Figs. 1 and 2). However, at 400°C (Fig. 3) a large solubility of about 8.5 at.% Sn was observed. This situation is rather unusual, as solubilities would be expected to decrease when going to lower temperature. However, there are some experimental phase diagrams showing a very similar shape of the (Cu,Ni) phase field, e.g., Chen et al.[17] Despite this the large solubility was drawn using dashed lines in Fig. 3 of the present work.

In both binary systems, the phases Cu_6Sn_5 HT and Ni_3Sn_2 HT have an $InNi_2$-type structure, a partially filled variant of the NiAs type. As this structure type is extremely flexible,[28] a large number of phases with NiAs superstructures exist in the two binaries: three different orthorhombic Ni_3Sn_2 LT phases (see Refs. 4 and 8–11) and three monoclinic Cu_6Sn_5 superstructures: Cu_6Sn_5 LT (η'-Cu_6Sn_5 according to Ref. 23), η^6-Cu_5Sn_4 and η^8-Cu_5Sn_4.[24] Since a continuous ternary solid solution is only possible for phases with isotypic crystal structures, a corresponding continuous solution $(Cu,Ni)_3Sn_2$ could theoretically only exist for the two HT phases in a small concentration and temperature range. In the literature,[16–19] small two-phase fields were reported between the Ni_3Sn_2 and Cu_6Sn_5 phases without specifically taking into account the various LT modifications. While practically all of the literature reports extended ternary solubilities of both binary phases, Oberndorff et al. mentioned a small solubility of Ni in Cu_6Sn_5 at 235°C and postulated the existence of a ternary compound around $Cu_{27}Ni_{29}Sn_{44}$.[21] This is in contrast to other phase diagram versions published up to now. The present results, too, support an extended solubility range of Cu_6Sn_5 HT (Figs. 3 and 4).

At 400°C the ternary solution of Cu_6Sn_5 HT was observed in all relevant samples, but none of the other related superstructure phases reported in the literature. There was no indication of a ternary compound in this region. However, various Ni_3Sn_2

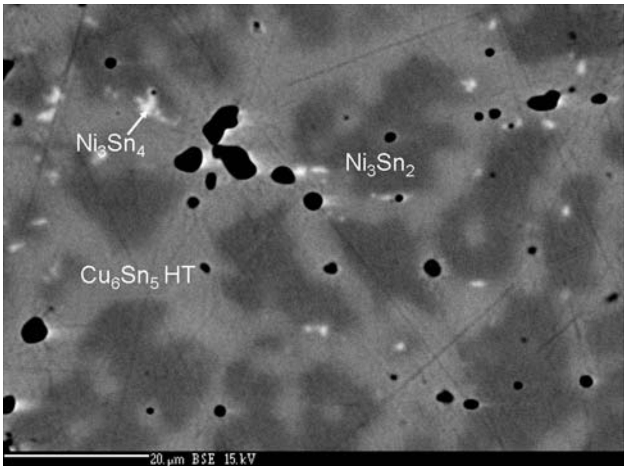

Fig. 7. SEM image of sample $Cu_{20}Ni_{37.5}Sn_{42.5}$ annealed at 220°C showing three phases: Ni_3Sn_2 LT or LT′ (*dark*), Cu_6Sn_5 HT (*medium*) and small amounts of Ni_3Sn_4 (*white*). The *black spots* are holes.

modifications were observed by XRD along its ternary solubility range (Table I). The predominantly observed phase was the HT phase with $InNi_2$-type structure. In some samples, however, the corresponding equilibrium phase was Ni_3Sn_2 LT or LT′, where it is rather difficult to distinguish these two structures in XRD powder patterns. For simplicity, it was decided to show the ternary solubility of Ni_3Sn_2 without indication of the different modifications, although the overall phase field of Ni_3Sn_2 could be experimentally evaluated based on EPMA. In Figs. 2–4, the inner part of the Ni_3Sn_2 area is therefore shown shaded.

At temperatures of 400°C and 220°C (Figs. 3 and 4), two- and three-phase fields, respectively, between Ni_3Sn_2 and Cu_6Sn_5 were observed by XRD, EPMA, and metallography. As an example Fig. 7 shows an SEM image of the microstructure of a sample $Cu_{20}Ni_{37.5}Sn_{42.5}$ annealed at 220°C, where the Ni_3Sn_2, Cu_6Sn_5 HT, and Ni_3Sn_4 phases can clearly be distinguished. At this temperature the XRD patterns of samples placed at $Cu_{10}Ni_{48}Sn_{42}$, $Cu_{20}Ni_{37.5}Sn_{42.5}$, and $Cu_{30}Ni_{26.5}Sn_{43.5}$ showed different additional line patterns, which could not be indexed using any of the known phases in this composition range. However, the appearance of additional lines in the XRD patterns is no proof for the existence of ternary compounds in this concentration range, because analysis of these samples was complicated by two facts: (1) due to the change of the cell dimensions in the ternary solid solutions, reflexes shift in the XRD patterns. A clear distinction of complex XRD patterns of closely related structures is hardly possible; (2) the homologous annealing temperature of 220°C (or even 400°C) is low; samples were therefore slowly cooled to this temperature prior to annealing to approach the equilibrium gradually. Nevertheless the establishment of equilibrium cannot be assured. This is especially true for (Cu,Ni)-rich alloys with a Sn content below 40 at.%. Thus the phase relations in this part of the isothermal section at 220°C had to be derived in analogy to the results at 400°C. They are therefore shown in a lighter shade of grey (Fig. 4).

The solubility of Cu in Ni_3Sn_4 was found to be much smaller than in the other Ni-Sn phases. It varies between 3.6 at.% at 700°C and 5.6 at.% at 220°C. Measurements of the solubility of Cu and Ni in (Sn) were complicated by the development of fine microstructures of (Sn) and Cu_6Sn_5 (e.g., samples $Cu_{20}Ni_{20}Sn_{60}$ and $Cu_{10}Ni_{30}Sn_{60}$ annealed at 220°C); however, according to our data and in consistency with the solubility in the binary systems this ternary solubility is negligible.

CONCLUSIONS

A set of isothermal sections at 220, 400, 500, and 700°C is presented for the ternary Cu-Ni-Sn system. A number of serious uncertainties in the literature could be clarified based on a careful study of the available literature and our own experimental work, resulting in a description different from recent reports. Furthermore the existence of two ternary compounds as proposed by Lee Pak et al.[14] around 25 at.% Sn, $\tau 1$ (βCu_3Ti-type structure) and $\tau 2$ (triclinic, distorted $\tau 1$), could be confirmed in this work. Other ternary compounds reported in the literature, $NiCu_2Sn$ (Häusler phase),[20] $Cu_4Ni_2Sn_5$,[22] and $Cu_{27}Ni_{29}Sn_{44}$[21] could not be confirmed and were therefore not accepted for the isothermal sections.

ACKNOWLEDGEMENTS

This research is a contribution to the European COST Action MP-0602. Financial support of the Austrian Science Foundation (FWF) under Project No. P-16495-N11 is gratefully acknowledged. The authors also want to thank Dr. Ales Kroupa (Institute of Physics of Materials, ASCR, Brno) for help with SEM/EDX measurements, and Marta Rodríguez-Hortalá, Melchior Camus, and Usman Saeed for their experimental contributions to this work.

REFERENCES

1. D.J. Chakrabarti, D.E. Laughlin, S.W. Chen, and Y.A. Chang, *Phase Diagrams of Binary Nickel Alloys*, ed. P. Nash (Materials Park, OH: ASM International, 1991).
2. T.B. Massalski, H. Okamoto, P.R. Subramanian, and L. Kacprzak, *Binary Alloy Phase Diagrams* (Materials Park, OH: ASM International, 1991).
3. N. Saunders and A.P. Miodownik, *Bull. Alloy Phase Diagr.* 11, 278 (1990).
4. C. Schmetterer, H. Flandorfer, K.W. Richter, U. Saeed, M. Kauffman, P. Roussel et al., *Intermetallics* 15, 869 (2007). doi:10.1016/j.intermet.2006.10.045.
5. A. Nash and P. Nash, *Bull. Alloy Phase Diagr.* 6, 350 (1985). doi:10.1007/BF02880521.
6. G. Ghosh, *Metall. Mater. Trans.* 30A, 1481 (1999). doi:10.1007/s11661-999-0085-x.
7. H.S. Liu, J. Wang, and Z.P. Jin, *Calphad* 28, 363 (2005). doi:10.1016/j.calphad.2004.12.002.
8. A. Leineweber, M. Ellner, and E.J. Mittemeijer, *J. Solid State Chem.* 159, 191 (2001). doi:10.1006/jssc.2001.9150.
9. A. Leineweber, O. Oeckler, and U. Zachwieja, *J. Solid State Chem.* 177, 936 (2004). doi:10.1016/j.jssc.2003.09.033.

10. A. Leineweber, *J. Solid State Chem.* 177, 1197 (2004). doi:10.1016/j.jssc.2003.10.028.
11. A. Leineweber, E.J. Mittemeijer, M. Knapp, and C. Baehtz, *Mater. Sci. Forum* 443–444, 247 (2004).
12. G. Ghosh, *Landolt Bernstein, New Series IV/11C3*, MSIT (Berlin - Heidelberg: Springer, 2007), 303 p.
13. E. Wachtel and E. Bayer, *Z. Metallk.* 75, 61 (1984).
14. J.S. Lee Pak, K. Mukherjee, O.T. Inal, and H.-R. Pak, *Mater. Sci. Eng. A* 117, 167 (1989). doi:10.1016/0921-5093(89)90098-1.
15. J.S. Lee Pak, K. Mukherjee, O.T. Inal, and H.-R. Pak, *Mater. Sci. Eng. A* 130, 83 (1989). doi:10.1016/0921-5093(90)90083-F.
16. C.-H. Lin, S.-W. Chen, and C.-H. Wang, *J. Electron. Mater.* 31, 907 (2002). doi:10.1007/s11664-002-0182-8.
17. W.T. Chen, C.E. Ho, and C.R. Kao, *J. Mater. Res.* 17, 263 (2002). doi:10.1557/JMR.2002.0036.
18. C.-Y. Li and J.-G. Duh, *J. Mater. Res.* 20, 3118 (2005). doi:10.1557/JMR.2005.0391.
19. C.-Y. Li, G.-J. Chiou, and J.-G. Duh, *J. Electron. Mater.* 35, 343 (2006). doi:10.1007/BF02692455.
20. W.H. Schreiner, P. Pureur, T.A. Grandi, J.V. Kunzler, and D.E. Brandão, *J. Therm. Anal.* 17, 489 (1979). doi:10.1007/BF01914037.
21. P. Oberndorff (PhD thesis, Technical University Eindhoven, 2001) 75 p.
22. C. Yu, J. Liu, H. Lu, P. Li, and J. Chen, *Intermetallics* 15, 1471 (2007). doi:10.1016/j.intermet.2007.05.005.
23. A.-K. Larsson, L. Stenberg, and S. Lidin, *Acta Crystallogr. B* 50, 636 (1994). doi:10.1107/S0108768194004052.
24. A.-K. Larsson, L. Stenberg, and S. Lidin, *Z. Kristallographie* 210, 832 (1995).
25. P. Villars, and L.D. Calvert, *Pearson's Handbook of Crystallographic Data for Intermetallic Phases* (Materials Park, OH: ASM International, 1991).
26. C. Schmetterer, M. Rodríguez-Hortalá, H. Flandorfer, and H. Ipser (University of Vienna, 2008), work in progress.
27. H. Knödler, *Metallurgist* 18, 1172 (1964).
28. S. Lidin and A.-K. Larsson, *J. Solid State Chem.* 118, 313 (1995). doi:10.1006/jssc.1995.1350.
29. J. Miettinen, *Calphad* 27, 309 (2003). doi:10.1016/j.calphad.2003.10.001.
30. C.-H. Wang and S.-W. Chen, *Metall. Mater. Trans. A* 34A, 2281 (2003). doi:10.1007/s11661-003-0292-9.